ELSEVIER

Chemical Geology 200 (2003) 377–393

CHEMICAL GEOLOGY
INCLUDING
ISOTOPE GEOSCIENCE

www.elsevier.com/locate/chemgeo

Solubility of the assemblage albite+K-feldspar+andalusite+quartz in supercritical aqueous chloride solutions at 650 °C and 2 kbar

Tatyana M. Pak[a], Christoph A. Hauzenberger[b,*], Lukas P. Baumgartner[b,1]

[a] *Department of Geology and Geophysics, University of Wisconsin, USA*
[b] *Institut für Geowissenschaften, Universität Mainz, Germany*

Received 1 October 2002; accepted 6 June 2003

Abstract

The solubility of the high grade pelite assemblage albite + K-feldspar + andalusite + quartz at 650 °C and 2 kbar was determined in aqueous solutions over a total chloride range of 0.01–3 m_{Cl}^{tot} using rapid-quench hydrothermal technique. The concentration of Na, K, Si, and Al was determined in the fluid phase after quench. The K/Na ratio was determined by approaching the equilibrium from below and above. It is 0.34 at low chloride concentrations and decreases slightly to 0.31 with increasing total chloride. Silica and aluminum concentrations were determined only from undersaturation. The silica solubility is found to be independent of chloride concentration and is ~ 0.13 molal. Aluminum is nearly independent of chloride concentration decreasing only slightly from ~ 0.0015 to ~ 0.0007 molal. Comparison of the experimental data with thermodynamic model calculations demonstrates that the silica concentrations are well predicted, while significant differences exist between individual databases for Al speciation and its total concentration. Al concentrations are underestimated by up to 10 to 15 orders of magnitude using the SUPCRT92 database. Predicted K/Na ratios are underestimated by up to 30%. The best predictions achieved for this simplified high-grade pelite assemblage are those using the SUPCRT92 database with revised thermodynamic data for feldspars and K- and Na-species (J. Phys. Chem. Ref. Data 24 (1995) 1401) and additional Al-species (Am. J. Sci. 295 (1995) 1255; Geochim. Cosmochim. Acta 61 (1997) 2175). The use of ideal mixing for neutral complexes in combination with the extended Debye–Hückel activity model for the charged species yields the most compatible speciation model.

Keywords: Solubility; Supercritical; Chloride solutions; Albite; K-feldspar

1. Introduction

Fluid infiltration during metamorphism has been recognized as an important driving force in contact and regional metamorphism during the last two decades (e.g. Ferry, 1988; Dipple et al., 1990; Ague, 1991, 1994a,b; Manning, 1997; Lasaga et al., 2001). Ague (1991, 1994a,b, 1997a,b) argued in a series of papers that extensive mass transfer occurs during regional metamorphism in pelites. Alkali chlorides

* Corresponding author. Present address: Institut für Mineralogie Kristallographie und Petrologie, Karl-Franzens-Universität Graz, Universitatsplatz 2, Graz 8010, Austria. Fax: +43-316-380-9865.

E-mail addresses: christoph.hauzenberger@uni-graz.at (C.A. Hauzenberger), Lukas.Baumgartner@img.unil.ch (L.P. Baumgartner).

[1] Present address: Institute of Mineralogy and Petrology, University Lausanne, Switzerland.

0009-2541/$ - see front matter © 2003 Elsevier B.V. All rights reserved.
doi:10.1016/S0009-2541(03)00211-0

are the principal solutes found in metamorphic rocks (e.g. Roedder, 1984; Banks et al., 1991; Ridley and Diamond, 2000). Hence, understanding the solubility of alkali-bearing silicates is a key to understanding alkali metal transport during metamorphism. Feldspars are major rock-forming minerals in the crust, and, together with micas, are the dominant alkali-metal-bearing silicates. We present experimental solubility data on the assemblage andalusite (And) + K-feldspar (Kfs) + albite (Ab) + quartz (Qtz) at 650 °C and 2 kbar and compare them with available thermodynamic data for solutes and minerals (Helgeson et al., 1978, 1981; Sverjensky et al., 1991, 1997; Johnson et al., 1992; Shock and Helgeson, 1988; Shock et al., 1989, 1992, 1997; Oelkers et al., 1995; Pokrovskii and Helgeson, 1995, 1997). Hauzenberger et al. (2001) presented solubility data using the similar mineral assemblage And + Kfs + Ab + Qtz. These experiments were done at a lower temperature of 600 °C and 2 kbar. He demonstrated that only experiments with a fully buffered mineral assemblage (e.g., And + Kfs + Ab + Qtz) give meaningful results.

The used mineral assemblage, And + Kfs + Ab + Qtz, is a typical assemblage for high-grade metapelites in contact aureoles. The results of this study are directly applicable to high-grade metamorphism of shallow crustal rocks.

2. Previous work

Many workers have studied the solubility of micas and feldspars in aqueous solutions (e.g. Hemley, 1959, 1967; Orville, 1963; Anderson and Burnham, 1963; Burnham, 1967; Beswick, 1973; Shade, 1974; Montoya and Hemley, 1975; Lagache and Weisbrod, 1977; Popp and Frantz, 1980; Gunter and Eugster, 1980; Wintsch et al., 1980; Vidale, 1983; Anderson and Burnham, 1983; Anderson et al., 1987; Woodland and Walther, 1987; Sverjensky et al., 1991; Baumgartner, 1992; Walther and Woodland, 1993; Shinohara and Fujimoto, 1994; Roux and Hovis, 1996; Hauzenberger et al., 2001). Of these studies, only a few include both Na- and K-silicates (Orville, 1963; Hemley, 1967; Burnham, 1967; Lagache and Weisbrod, 1977; Vidale, 1983; Anderson et al., 1987, Hauzenberger et al., 2001).

The pH of supercritical solutions have a profound influence on speciation and total metal concentration (Barnes, 1981; Anderson et al., 1987; Eugster and Baumgartner, 1987; Oelkers and Helgeson, 1991; Roselle and Baumgartner, 1995; Walther, 1997). In principal, the pH can be calculated by solving the charge balance equation for H^+, if all the solute concentrations have been measured (Roselle and Baumgartner, 1995). This follows from the fact, that the degree of freedom for a closed system with known composition at fixed pressure and temperature is equal to zero (e.g. Spear, 1993). A practical problem arises, because the concentration of H^+ is typically several orders of magnitude smaller than the individual solute concentrations. Hence, calculation of pH through charge balance from total solute concentrations requires extremely precise measurements for all the solute concentrations. In practice, this is not achievable. Hence, the pH of a solution has to be buffered by the mineral assemblage (Barnes, 1981; Eugster et al., 1987; Hauzenberger et al., 2001). This in turn requires a careful design of the solubility experiment so as to satisfy the requirement of thermodynamic buffering of the solution with respect to all components (Barnes, 1981; Eugster et al., 1987; Hauzenberger et al., 2001). The phase assemblage has to be chosen to constrain the chemical potential of each component. Alternatively, the chemical potential of a component has to be measured if not imposed by the assemblage.

The experiments reported by Vidale (1983), Anderson et al. (1987), and Hauzenberger et al. (2001) are the only completely buffered experiments. No data is available at 650 °C which corresponds to the upper stability limit of this mineral assemblage without melting. Anderson et al. (1987) worked mostly on either a pure Na or K system. Their lone results at 600 °C and 2 kbar for two feldspars unfortunately did not contain sanidine after the experiment and, as a consequence, buffering is questionable. Hauzenberger et al. (2001) investigated the solubility of the same mineral assemblage at 600 °C and 2 kbar with varying total chloride concentration. The K/Na ratio for low chloride concentration ($Cl^{tot} = 0.05 - 1$ molal) is 0.33. It decreases to 0.28 at 3 molal total chloride concentration.

In the last three decades, much progress has been achieved in understanding the thermodynamics of inorganic aqueous species (Helgeson et al., 1981;

Tanger and Helgeson, 1988; Shock et al., 1989, 1992, 1997; Oelkers and Helgeson, 1990, 1991, 1993; Sverjensky et al., 1991; Johnson et al., 1992; Pokrovskii and Helgeson, 1995, 1997; Oelkers et al., 1995; Holland and Powell, 1998). The solubility of alkali feldspars in chloride solution constitutes an excellent test of thermodynamic databases, since the entropy and volume change of the principle reaction

$$\text{Albite (Ab)} + \text{KCl} \Leftrightarrow \text{K–feldspar (Kfs)} + \text{NaCl} \quad (1)$$

are very small (Dipple and Ferry, 1992). This makes the prediction of the pressure and temperature dependence for the equilibrium constant highly sensitive to small errors in the thermodynamic databases for minerals and solutes.

3. Experimental method

Experiments were performed using the cold-seal rapid quench hydrothermal technique (Tuttle, 1949; Wellman, 1970). This technique allowed runs to be quenched to room temperature in a few seconds, while pressure is released within approximately 30 seconds. A total solid charge of 20–40 mg of solids was loaded together with ~ 100 μl of fluid into a 3-cm-long gold tube with 4 mm diameter. The gold tube was welded shut with a carbon arc welder and the capsule was checked for leakage by heating it to 110 °C for approximately 2 hr. Capsules with a weight loss of more than 0.1 mg were discarded.

Argon was used as the pressure medium and the whole assembly (furnace and vessel) was tilted at approximately 5° to minimize temperature gradients (Rudert et al., 1976). Temperature was controlled by Eurotherm 815 PID controllers using Nicrosil–Nisil thermocouples inserted in the external thermocouple well at the back end of the pressure vessel. The temperature for each experiment was monitored by computer on average every 30 min. Pressure was measured with a factory calibrated Precise Sensor strain gauge, and checked against a Heise-Bourdon pressure gauge. The accuracy of the temperatures is estimated to be ± 5 °C. Pressure was maintained within ± 20 bars for individual runs and is estimated to be accurate to within ± 50 bars.

Natural low albite from Amelia, Virginia, and natural microcline from a pegmatite, Black Hills, S. Dakota, were exchanged with NaCl and KCl, respectively, at 900 °C for 48 h following Orville's (1963) procedure. Exchanged feldspars were examined by X-ray diffraction to verify the low ordering state (Orville, 1967) and analyzed with a Cameca SX-50 microprobe (Table 1). Natural andalusite from Andalusia, Spain (Table 1) and natural quartz (University of Wisconsin-Madison Museum collection) were cleaned in a boiling 5% HCl solution and then carefully rinsed in ultrapure water (Barnstead nanopure ultrapure water system, #D4741). Based on initial trials, a molar ratio for Ab/Kfs/Qtz/And of approximately 6:2:8:1 was selected. The starting mix was ground in alcohol until a homogeneous, fine-grained powder was obtained (average grain size ~ 20–50 μm). Solid products were examined by microscope, X-ray powder diffraction and electron microprobe (Cameca SX-50). No minerals other than the starting mineral phases were found. All runs listed in Table 2 contain the four mineral phase assemblage.

Starting solutions were prepared using de-ionized ultrapure water and variable amounts of NaCl (lot#914194), KCl (lot#960801A), and HCl. The range in the Cl-content used (0.01 to ~ 3 m) reflects the typical salinity of metamorphic fluid inclusions. The upper chlorinity was limited by the one phase field for H_2O–NaCl–KCl solutions (Sterner et al., 1988, 1992). Starting solution compositions were prepared to achieve reversals in the K/Na ratio and the starting pH was chosen to bracket quench pH. No

Table 1
Microprobe analyses of starting material

	Low albite	Microcline	Andalusite
# Analyses	11	9	5
SiO_2	69.50 ± 0.2	64.86 ± 0.2	36.68
Al_2O_3	19.48 ± 0.1	18.30 ± 0.1	62.1
FeO	n.d.	n.d.	0.23
CaO	0.20 ± 0.1	n.d.	n.d.
Na_2O	11.18 ± 0.3	n.d.	n.d.
K_2O	0.16 ± 0.1	16.92 ± 0.1	n.d.
Total	100.52	100.09	99.01
Si	3.012	3.002	1.000
Al	0.995	0.998	1.995
Fe	0.000	0.000	0.005
Ca	0.009	0.000	0.000
Na	0.939	0.000	0.000
K	0.009	0.999	0.000

n.d. = not detected.

Table 2
Experimental data for the assemblage albite + K-feldspar + andalusite + quartz at 650 °C and 2 kbar

Duration			Starting solutions					Quench solutions							Charge balance	
n	Run Nr.	Days	Na^{tot}	K^{tot}	K/Na	Cl^{tot}	pH	Cl^{tot}	pH	Na^{tot}	K^{tot}	Al ($\times 10^{-4}$)	Si^{tot}	K/Na	%	
1	29	7	0.0074	0.0015	0.197	0.010	3.52	0.010	4.03	0.0207	0.0072	3.4	0.108	0.349	49	x
2	69	12	0.0024	0.0008	0.320	0.003	3.87	0.014	4.90	0.0084	0.0027	11.5	0.122	0.321	2	
3	70	12	0.0049	0.0018	0.376	0.010	3.54	0.017	4.90	0.0112	0.0037	7.4	0.0810	0.336	0	
4	30	7	0.0218	0.0048	0.218	0.022	3.26	0.022	4.05	0.0264	0.0092	4.5	0.162	0.349	25	x
5	80	25	0.0084	0.0018	0.213	0.012	3.21	0.023	3.90	0.0136	0.0050	15.6	0.152	0.364	1	
6	59	18	0.0042	0.0017	0.406	0.026	7.81	0.027	4.62	0.0164	0.0055	8.8	0.129	0.335	− 5	
7	31	7	0.0215	0.0041	0.190	0.028	3.56	0.028	3.97	0.0288	0.0100	2.5	0.0845	0.348	17	
8	53	14	0.0098	0.0023	0.231	0.018	3.63	0.035	5.70	0.0234	0.0083	4.9	0.0915	0.354	− 3	
9	71	12	0.0167	0.0063	0.379	0.028	3.57	0.044	4.10	0.0234	0.0078	5.3	0.166	0.334	− 14	
10	60	18	0.0178	0.0066	0.367	0.022	3.67	0.048	3.98	0.0302	0.0101	5.9	0.133	0.335	− 6	
11	33	7	0.0207	0.0041	0.197	0.073	3.39	0.073	3.79	0.0620	0.0210	2.7	0.0466	0.339	7	
12	81	25	0.0750	0.0288	0.383	0.107	2.63	0.121	3.00	0.0784	0.0301	14.6	0.148	0.383	− 3	
13	34	7	0.164	0.0250	0.152	0.196	2.48	0.196	2.52	0.137	0.0476	2.6	0.0988	0.348	− 2	
14	61	18	0.0978	0.0447	0.457	0.159	3.32	0.197	2.73	0.117	0.0419	6.1	0.178	0.359	− 10	
15	55	14	0.168	0.0399	0.238	0.258	3.64	0.247	3.20	0.165	0.0533	5.1	0.118	0.323	− 6	
16	75	15	0.0886	0.0352	0.397	0.153	3.28	0.278	2.50	0.0483	0.0171	7.6	0.168	0.353	− 59	x
17	62	18	0.179	0.0710	0.395	0.286	2.27	0.322	2.54	0.198	0.0640	6.8	0.154	0.323	− 9	
18	56	14	0.327	0.0797	0.243	0.533	3.33	0.471	2.20	0.306	0.0974	7.1	0.185	0.318	− 7	
19	35	7	0.535	0.0492	0.092	0.526	3.26	0.526	1.97	0.406	0.128	2.0	0.109	0.316	2	
20	36	7	0.453	0.0822	0.182	0.610	2.26	0.610	1.98	0.408	0.132	2.6	0.0975	0.324	− 5	
21	76	15	0.346	0.142	0.411	0.541	2.21	0.889	2.00	0.192	0.0659	8.7	0.117	0.343	− 53	x
22	72	12	0.606	0.239	0.395	1.11	1.18	1.05	1.90	0.655	0.194	1.6	0.116	0.296	− 10	
23	63	18	0.554	0.216	0.390	0.792	1.57	1.20	1.84	0.634	0.209	6.9	0.154	0.330	− 16	
24	58	14	1.692	0.243	0.144	1.54	1.14	1.46	1.50	0.988	0.317	5.5	0.117	0.321	− 4	
25	57	14	1.662	0.235	0.142	2.33	1.04	2.37	1.30	1.626	0.427	0.4	0.0616	0.263	− 6	
26	77	15	1.703	0.736	0.432	2.75	1.27	2.66	1.50	0.996	0.355	12.3	0.0621	0.356	− 32	x
27	82	25	2.051	0.402	0.196	2.75	1.26	2.85	1.60	1.928	0.601	5.6	0.124	0.312	− 5	

Run Nr. = run number. Dur. = run duration in days. All values are given in molal.
Charge balance, %=[Cl − (Na + K + Al × 3 + 10 − pH)/(Cl + Na + K + Al × 3 + 10 − pH) × 100; x indicates runs with large charge in balance.

attempt was made to reverse the total concentration of Al and Si.

After quench, each capsule was punctured with a stainless steel needle in a glove box. The box was purged with water saturated Ar or N_2 to avoid evaporation of the fluid and dissolution of CO_2 in the fluid droplet. Solutions were extracted, centrifuged and diluted by mass for elemental analysis. The run solutions were analyzed for K and Na by flame atomic absorption spectroscopy. A Zeeman graphite furnace atomic absorption spectroscopy was used for Al and Si analysis (Perkin-Elmer model: 5100ZL). Total chloride concentration for each run was measured by silver titration using a Buchler Chloridometer. Estimated total relative uncertainties in Na and K, Al and Si, and total Cl are 5%, 15%, and 5%, respectively. These estimates include dilution, calibration and instrumental uncertainties. Quench pH was obtained using a microelectrode (model #: MI-410). Values reported are not corrected for the effect of solutes. The reported values are believed to be accurate within ~ 0.15 log units (Roselle and Baumgartner, 1995).

4. Experimental results

Experimental results for 650 °C and 2 kbar are reported in Table 2. The runs are arranged according to increasing total chloride concentrations. No systematic differences were observed for run times between 7 and 25 days. This suggests that equilibrium was closely approached already after 7 days at these P–T conditions. The run conditions of 650 °C and 2 kbar are just within the sillimanite stability field (Holdaway, 1971).

Since andalusite was used for the experiments, all runs were carefully checked for the presence of sillimanite by optical and/or X-ray investigations. No sillimanite was detected in any of the runs.

The charge balance was calculated assuming that Na, K, and Al-complexes completely dissociate upon quench to single ions, while Si was assumed to remain as the neutral H_4SiO_4 complex. Charge balance errors in excess of 15% to 20% indicate a faulty analysis or precipitation of ions from the fluid in the gold capsule during quench. Especially Al and Si can easily precipitate if the quench process will last longer than a few seconds. This happened, when the gold capsule could not slide freely from the hot to the cold part of the cold seal vessel. Analysis for five experiments (Table 2; runs # 29, 30, 75, 76, 77) resulted in large charge balance errors. These were excluded from the data set in the subsequent discussion.

Total concentrations of components are plotted against the total chloride concentration in Fig. 1. At low chloride concentrations, Si is the dominant solute. Na and Cl are the most abundant solutes, above a total chloride concentration of about 0.1 m. Na and K solubility increase linearly with a slope close to one. The sum of the alkali metal concentrations is within analytical error equal to the total chloride concentration.

Si and Al equilibrium concentrations were only approached from under saturation. Hence, the values reported here most likely represent minimum values. The solubility of Si was found to be independent of the total chloride concentration and is ~ 0.13 molal. The aluminum solubility seems to decrease slightly from ~ 0.0015 to ~ 0.0007 molal with increasing chloride concentration. However, the large scatter and uncertainty in aluminum concentration should be noted. The K/Na ratio is 0.34 ± 0.02 for total chloride concentrations up to 0.4 m, after which it starts to decrease slightly to 0.31 ± 0.02 (Fig. 2).

Quench pH decreases from above 6 to about 1.3 with increasing total chloride content (Table 2). Quench pH is a sensitive measure of the difference between cations and anions. It reflects the charge balance between the total anion concentration and the total cation concentration upon quench. Fig. 3 shows a plot of the ratio of total Na over quench H^+ as a function of the total chloride concentrations. Such plots have been used in the past to gain information on

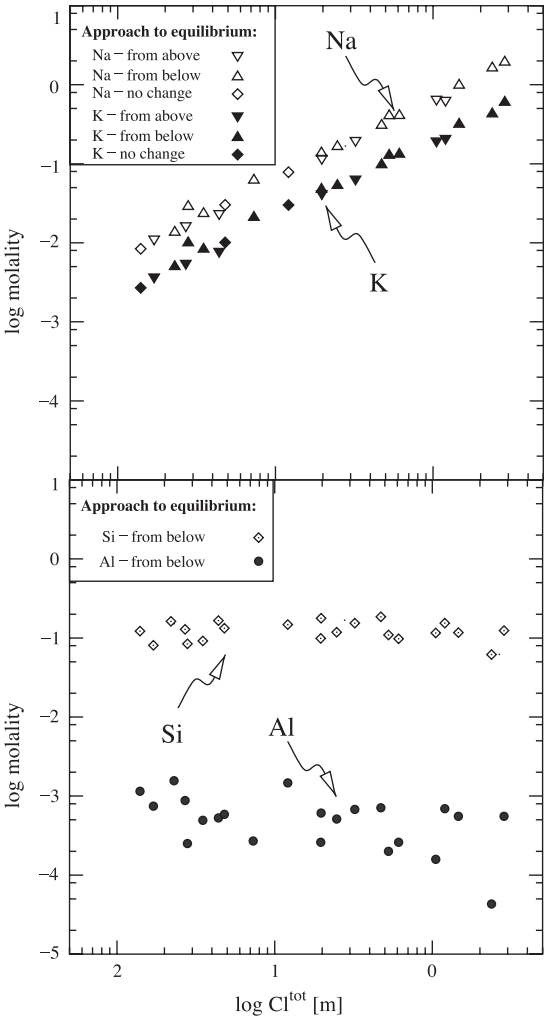

Fig. 1. Measured concentration of Si, Al, K and Na in chloride-rich solutions plotted as a function of the total chloride content for the assemblage albite (Ab) + K-feldspar (Kfs) + andalusite (And) + quartz (Qtz) at 650 °C and 2 kbar. The concentrations of Na and K were experimentally reversed, while Si and Al concentrations were approached from under saturation only.

the speciation in systems where one chloride complex dominates (e.g. Hemley, 1959; Wilson and Eugster, 1990; Roselle and Baumgartner, 1995). If sodium speciation changes with increasing chloride concentration, the Na^{tot}/H_q^+ ratio should change. The observed Na^{tot}/H_q^+ ratio is slightly decreasing with increasing Cl^{tot}. Therefore, some change in sodium speciation can be assumed (Fig. 3). For a detailed discussion of this type of graph, see Roselle and Baumgartner (1995).

To illustrate the meaning of quench pH, we assume that K and Na are completely associated as single chloride complexes (NaCl, KCl) at *P*, *T*, and that HCl is the only other chloride species present in solution. The equilibrium constant for the reactions

$$\mathrm{Ab} + \mathrm{HCl}^0 \Leftrightarrow \mathrm{NaCl}^0 + 0.5\ \mathrm{And} + 2.5\ \mathrm{Qtz} + 0.5\ \mathrm{H_2O} \quad (2a)$$

$$\mathrm{Kfs} + \mathrm{HCl}^0 \Leftrightarrow \mathrm{KCl}^0 + 0.5\ \mathrm{And} + 2.5\ \mathrm{Qtz} + 0.5\ \mathrm{H_2O} \quad (2b)$$

can be written as

$$\mathrm{K_{2a}} = \frac{a_{\mathrm{NaCl}^0}}{a_{\mathrm{HCl}^0}} \cong \frac{m_{\mathrm{NaCl}^0}}{m_{\mathrm{HCl}^0}} \cong \frac{m^{\mathrm{tot}}_{\mathrm{Na}}}{m_{\mathrm{H}^+_q}} \quad (3a)$$

$$\mathrm{K_{2b}} = \frac{a_{\mathrm{KCl}^0}}{a_{\mathrm{HCl}^0}} \cong \frac{m_{\mathrm{KCl}^0}}{m_{\mathrm{HCl}^0}} \cong \frac{m^{\mathrm{tot}}_{\mathrm{K}}}{m_{\mathrm{H}^+_q}} \quad (3b)$$

where m_i is the molality, a_i is the activity of species i. The subscript q designates the concentrations measured after quench. An activity coefficient of one was assumed for uncharged aqueous complexes. Eqs. (3a) and (3b) assume that the complexes of aluminum and silica do not contribute significantly to the room temperature charge balance equation. Then, m_{H^+} is equal to the H^+ concentration. As a consequence, the ratio of Na^{tot}_q to H^+_q on quench is constant, and one predicts a horizontal line in Fig. 3. Comparison with Fig. 3 reveals that the experimentally determined values decrease slightly with increasing total chloride concentration. This indicates that other alkali metal chloride species at very low and higher total chloride concentrations are present in the solution at run conditions.

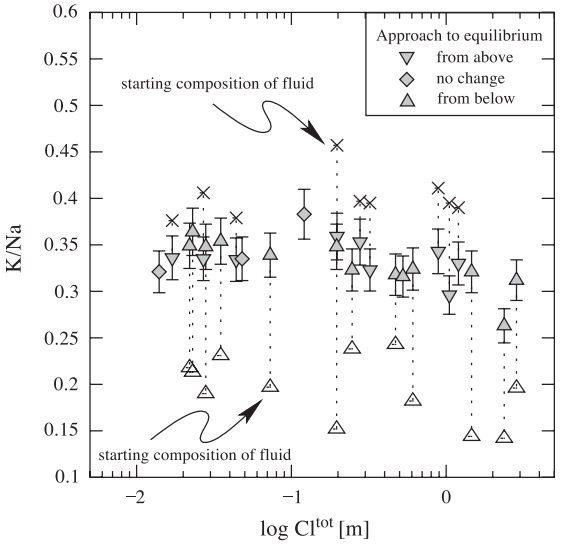

Fig. 2. The equilibrium K/Na ratio (both alkalis measured in molal units) in chloride solution for the assemblage Ab + Kfs + And + Qtz is plotted as a function of the total chloride content. The K/Na ratio is independent of the total chloride concentration. The slight apparent decrease at high chloride concentration is within experimental error. This suggests that the same Na- and K-species dominate over the entire range in chloride concentrations.

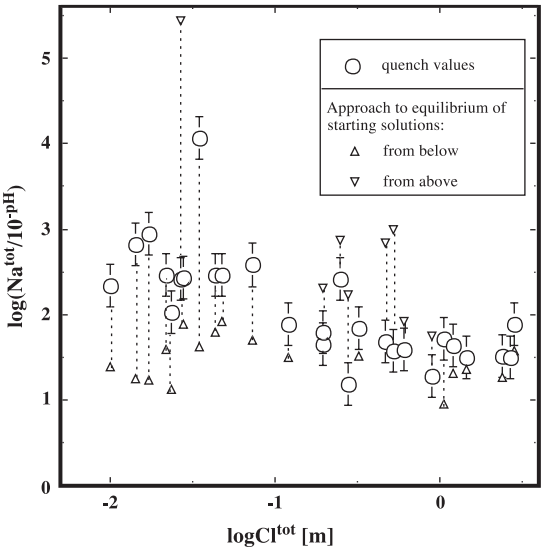

Fig. 3. Plot of the total Na concentration (molal) over quench H^+ as a function of the total chloride concentration in the fluid. Here, the *y*-axes value approximately equals the equilibrium constant of reaction (2a), assuming that the only chloride species are NaCl, KCl, and HCl. In this case, a horizontal line is predicted. The decrease in Na^+/H^+ from 0.01 to 0.1 Cl^{tot} indicates a change in speciation. At total chloride concentrations between 0.1 and 3, a near horizontal line in the Na^+/H^+ ratio shows that no dramatic change in Na speciation occurs at higher Cl^{tot} concentrations.

5. Modeling of the solubility experiments

5.1. Thermodynamic models

We modeled our experimental data set with thermodynamic data on aqueous species and minerals that are available in the literature. The thermodynamic data-

bases used in our calculations are summarized (in chronological order) in Table 3. The selection criteria for a database included: (a) the pressure and temperature of 2 kbar and 650 °C of the experiments is within the valid $P-T$ range quoted for the database; (b) the database is well documented and within the public domain; and (c) the database includes thermodynamic data for at least one complex for each major cation found in the solution. All of the data sets listed in Table 3 are based on a modified Born (1920) equation and the HKF-equation (Helgeson et al., 1981). The software package SUPCRT92 (Johnson et al., 1992) implements the HFK-equation and the subsequent improvements by Tanger and Helgeson (1988) and Shock et al. (1989, 1992). Its 1992 release includes a database (Johnson et al., 1992), which is referred to here as the SUPCRT92 database. It includes the Helgeson et al. (1978) mineral data set and the aqueous species database of Tanger and Helgeson (1988), Shock and Helgeson (1988), Shock et al. (1989), with further updates and corrections (Table 3). This database does not include thermodynamic data on the associated hydrogen chloride complex. There is a large discrepancy between dissociation constants derived from the conductivity experiments of Frantz and Marshall (1984) and that derived by Sverjensky et al. (1991) from solubility measurements. Nevertheless, data for HCl is crucial for any reasonable speciation models for supercritical solutions. We adopted the data of Sverjensky et al. (1991) in all our calculations, since these values were included in the subsequent releases of the same database.

The other databases are all based on SUPCRT92. For a detailed discussion of the individual databases, the reader is referred to the original publications (Table 3). Only a short review is given here to illustrate some of the differences. The Slop98 database includes, among other new data, a revised thermodynamic data set for Al. In addition, the thermodynamic data for the major K and Na species are revised (Table 3). The database is the revised SUPCRT92 thermodynamic database and is available over the World Wide Web from Shock.

The Svej91 data set (Sverjensky et al., 1991) contains modified thermodynamic data for KCl and KOH. The thermodynamic data for K-feldspar, microcline, muscovite and sanidine (Table 4) were adjusted to fit experiments on the solubility of muscovite and K-feldspar in aqueous solutions. Finally, the Po97 database (Pokrovskii and Helgeson, 1995, 1997; Oelkers et al., 1995) uses an expanded species set for aluminum. In addition, revised thermodynamic data for KCl, KOH, NaOH, as well as Na-, K- and Al-hydroxide species are given, along with revised thermodynamic properties for some alkali minerals.

Activity coefficients for charged aqueous species were calculated using the extended Debye–Hückel equation (Hückel, 1925; Bockris and Reddy, 1970; Helgeson et al., 1981):

$$\log\gamma_j = \frac{-(A_\gamma Z_j^2 I^{1/2})}{(1+\mathring{a}B_\gamma I^{1/2})}\Gamma_\gamma + \dot{b}I \qquad (4)$$

where $\mathring{a}$ is the ion size parameter, Z_j is the charge of ion j, A_γ and B_γ are the temperature- and pressure-dependent Debye–Hückel coefficients, and Γ_γ is the

Table 3
Thermodynamic databases used in the calculations

Databases	References	New Species	Minerals
SUPCRT92 (Sup92)	Johnson et al., 1992; Helgeson et al., 1978; Shock and Helgeson, 1988; Shock et al., 1989, 1992	H^+, OH^-, Cl^-, $NaCl^o$, Na^+, KCl^o, K^+, $H_4SIO_4^o$, $NaSi(OH)_5^o$, Al^{3+}, $Al(OH)^{2+}$, H_2O	
Svj91	Sverjensky et al., 1991	HCl^o, KCl^o, KOH^o	Kfs, Mi, Mu, San
Po97	Pokrovskii and Helgeson, 1995; Oelkers et al., 1995; Pokrovskii and Helgeson, 1997	Al^{3+}, $Al(OH)^{2+}$, $Al(OH)_2^+$, $Al(OH)_3^o$, $Al(OH)_4^-$, $NaAl(OH)_4^o$, $KAl(OH)_4^o$, $NaOH^o$, KOH^o, KCl^o	Ab, And, Mu, Mi, Kfs, San
Slop98	Shock et al., 1997; Sverjensky et al., 1997	Al^{3+}, $Al(OH)^{2+}$, $Al(OH)_2^+$, $Al(OH)_3$, $Al(OH)_4^-$, $NaOH^o$, KOH^o, KCl^o, $NaCl^o$, $NaSi(OH)_5^o$, Cl^-, HCl^o, H^+, OH^-, K^+, Na^+, $H_3SiO_4^-$	

Ab: albite; And: andalusite; Kfs: k-feldspar; Mi: microcline; Mu: muscovite; San: sanidine.

Table 4
Dissolution and dissociation/association reactions and used log K from various datasets for $T=650$ °C and $P=0.2$ GPa

Reaction #		SUP92, log K	PO97, log K	SLOP98, log K	SVJ91, log K
R1	1 Mic + 1 HCl = 1 KCl + 0.5 And + 2.5 Qtz + 0.5 H_2O	1.459	1.059[a]	1.480	1.410
R2[b]	1 San + 1 HCl = 1 KCl + 0.5 And + 2.5 Qtz + 0.5 H_2O	1.347	0.946[a]	1.368	1.297
R3	1 Kfsp + 1 HCl = 1 KCl + 0.5 And + 2.5 Qtz + 0.5 H_2O	1.318	0.918[a]	1.339	1.269
R4	1 Ab,low + 1 HCl = 1 NaCl + 0.5 And + 2.5 Qtz + 0.5 H_2O	2.391	1.769[a]	2.393	2.391
R5[b]	1 Ab,high + 1 HCl = 1 NaCl + 0.5 And + 2.5 Qtz + 0.5 H2O	2.371	1.749[a]	2.373	2.371
R6	1 Ab + 1 HCl = 1 NaCl + 0.5 And + 2.5 Qtz + 0.5 H_2O	2.250	1.629[a]	2.253	2.250
R7	0.5 And + 3 H^+ = 0.5 Qtz + 1 Al^{+3} + 1.5 H2O	− 5.675	− 6.514[a]	− 5.873	− 5.675
R8	1 Qtz = 1 SiO_2,aq	− 0.858	− 0.858[a]	− 0.858	− 0.858
R9	1 H2O = 1 H^+ + OH^-	− 11.204	− 11.204[a]	− 11.204	− 11.204
R10	1 HCl = 1 H^+ + Cl^-	− 4.204	− 4.204[a]	− 4.204	− 4.204
R11	1 NaCl = 1 Na^+ + Cl^-	− 2.338	− 2.338[a]	− 2.340	− 2.338
R12	1 KCl = 1 K^+ + Cl^-	− 2.036	− 2.043[c]	− 2.057	− 2.042
R13	1 $Al(OH)^{+2}$ = 1Al^{+3} + 1 OH^-	− 11.525	− 14.276[d]	− 13.265	− 11.525
R14	1 $Al(OH)_2^+$ = 1Al + ^{3} + 2 OH^-	–	− 25.634[d]	–	–
R15	1 AlO^+ + 1 H^+ = 1Al^{+3} + 1 OH^-	–	–	− 11.226	–
R16	1 $HALO_{2,aq}$ + 1 H2O = 1Al^{+3} + 3 OH^-	–	− 36.104[d]	− 31.270	–
R17	1AlO_2^- + 2 H2O = 1Al^{+3} + 4 OH^-	–	− 40.989[d]	− 40.322	–
R18	1 $KAlO_{2,aq}$ = 1 K^+ + 1AlO2$^-$	–	− 2.833[d]	–	–
R19	1 $NaAlO_{2,aq}$ = 1 Na^+ + 1AlO2$^-$	–	− 3.345[d]	–	–
R20	$NaHSiO_{3,aq}$= 1 Na^+ + 1 OH^- + 1 $SiO_{2,aq}$	− 1.850	− 1.850[a]	− 1.945	− 1.850
R21	$HSiO_3^-$ = 1 $SiO_{2,aq}$ + OH^-	–	0.069[a]	− 0.165	–
R22	1 KOH = 1 K^+ + 1 OH^-	–	− 2.622[a]	− 1.515	− 2.585
R23	1 NaOH = 1 Na^+ + 1 OH^-	–	− 3.600[a]	− 1.167	–

The Debye–Hückel equation for charged species was used for speciation calculations for all databases.
SUP92 = Johnson et al. (1992).
SLOP98 = Shock (1998).
SVJ91 = Sverjensky et al., 1991.
[a] PO97: = Oelkers et al., 1995.
[b] The activity of disordered feldspars was calculated using the mixing model of Fuhrman and Lindsley (1988).
[c] PO97: = Pokrovskii and Helgeson, 1997.
[d] PO97: = Pokrovskii and Helgeson, 1995.

mole fraction to molality conversion factor. $\dot{b}$ is the extended term parameter for the charged species j and I the ionic strength. The mixing behavior for neutral species was either assumed to be ideal, or, alternatively was calculated using the Setchenow equation (Setchenow, 1892; Oelkers and Helgeson, 1991):

$$\log\gamma_j = \dot{b}_n I \quad (5)$$

where $\dot{b}_n$ is the Setchenow coefficient for neutral species.

The choice of the best value for the species dependent parameters—ion size, Debye–Hückel extended term and Setchenow coefficients—is difficult in the case of multi-component solutions (Brimhall and Crerar, 1987). Here, we made the common assumption that the dominant solute determines these interaction parameters (Helgeson et al., 1981; Brimhall and Crerar, 1987). Hence, the activity coefficients for charged and neutral alkali species were calculated using the parameters for NaCl° ($\mathring{a}$, $\dot{b}$, $\dot{b}_n$) of Helgeson et al. (1981) and Oelkers and Helgeson (1991, 1993).

Activities of mineral phases were assumed to be one in most calculations, because the starting mineral compositions are very close to end member compositions (Table 1). Low feldspars were used in the experiments, because experimental studies indicate, that their ordering state remains unchanged during these relatively short-term hydrothermal experiments (e.g. Orville, 1963; Martin, 1969). However, we observed newly grown rims on feldspars in many, but not all, experiments as products. Thin rims (up to 10 μm) of either albite on K-feldspar or K-feldspar

on albite grains were detected. When the K/Na ratio was approached from high values, i.e. excess of K in solution, mostly rims of K-feldspar were observed on albite grains. Alternatively, mostly rims of albite were detected on K-feldspar, when the K/Na ratio was approached from below the equilibrium. The compositions of these rims were difficult to measure because of their size (>10 mm). Nevertheless, considerable solid solution between K-feldspar and albite was observed in these rims (albite rim: X_{ab} = 0.716; K-feldspar rim: X_{ab} = 0.392). Hence, we performed additional calculations. We assumed that the rims dominated the solubility of the feldspars. Feldspar solid solution activities were calculated using the Fuhrman and Lindsley (1988) feldspar mixing model (albite rim: a_{ab} = 0.905; K-feldspar rim: a_{Kfs} = 0.717). Disordered feldspar thermodynamic data were used, since precipitates are likely disordered (Martin, 1969).

5.2. Speciation calculations

The speciation and total ion concentrations of the supercritical fluid phase in equilibrium with the experimental mineral assemblage were calculated by solving the equations describing the equilibrium between the minerals and aqueous species, the charge balance equation, and the total chloride concentration (Wolery, 1979; Eugster and Baumgartner, 1987). A set of independent reactions for the equilibrium between the chloride-bearing aqueous solutions and the mineral assemblage Ab + Kfs + And + Qtz is given in Table 4 using all species present in a specific database. The reactions were written with the basis species which are common to all databases. This way it is easy to compare the thermodynamic data. The FORTRAN code SOLUBLE (Roselle and Baumgartner, 1995), based on the Newton–Raphson iteration (Wolery, 1979; Eugster and Baumgartner, 1987), was used to solve the nonlinear set of equations. Basis set switching (Wolery, 1979) was performed manually to ensure convergence of the solution algorithm.

Nearly 200 combinations are possible for the options discussed above. These include *four* databases (Sup92, Slop98, Sverj91, Po97), *three* different ordering state assumptions for each feldspar (completely ordered or disordered, stable ordering state), *two* different activity–composition relationships for the feldspars (pure phases, activity model of Fuhrman and Lindsley, 1988), *two* activity–composition relationships for charged solutes (Debye–Hückel, extended Debye–Hückel), and *two* activity–composition relationships for neutral species (ideal mixing, Setchenow law). Not all of these combinations are equally reasonable. We selected combinations that are thermodynamically compatible. These included the assumption that (a) newly grown feldspars are disordered while the ordering state of the starting feldspar is not changed (Orville, 1963; Martin, 1969); that the (b) thermodynamic data for albite and K-feldspar are calculated both for the same ordering state and activity–composition relationship, and (c) the Setchenow equation for neutral solutes is best matched with the extended Debye–Hückel equation. For each database, all the species present were used. The uncharged solute species are modeled, unless otherwise stated, as an ideal solution, while charged complexes were modeled using the Debye–Hückel equation.

We present a summary of the calculations in the following sections. No effect on the solubility of Si and only very small changes on the solubility of Al are predicted by changing the order parameter and solid-solution properties of the feldspars. The ordering state and solid-solution properties, however, do influence the K/Na ratio, and these effects are discussed in detail below.

6. Comparison of the experimental data with the thermodynamic models

6.1. Silica

Si concentrations are well predicted by all databases (Fig. 4a–d). The Si solubility in our experiments was always buffered by the dissolution or precipitation of quartz. It is generally agreed that Si solubility is dominated in neutral to acidic solutions by the uncharged hydroxide species, $H_4SiO_4^0 \cdot nH_2O$, where n equals 2 to 4, the number of water molecules in the first hydration shell (Walther and Helgeson, 1977; Walther and Orville, 1983; Walther, 1986; Eugster and Baumgartner, 1987; Manning, 2001). The single de-protonated silicic acid species ($H_3SiO_4^-$)

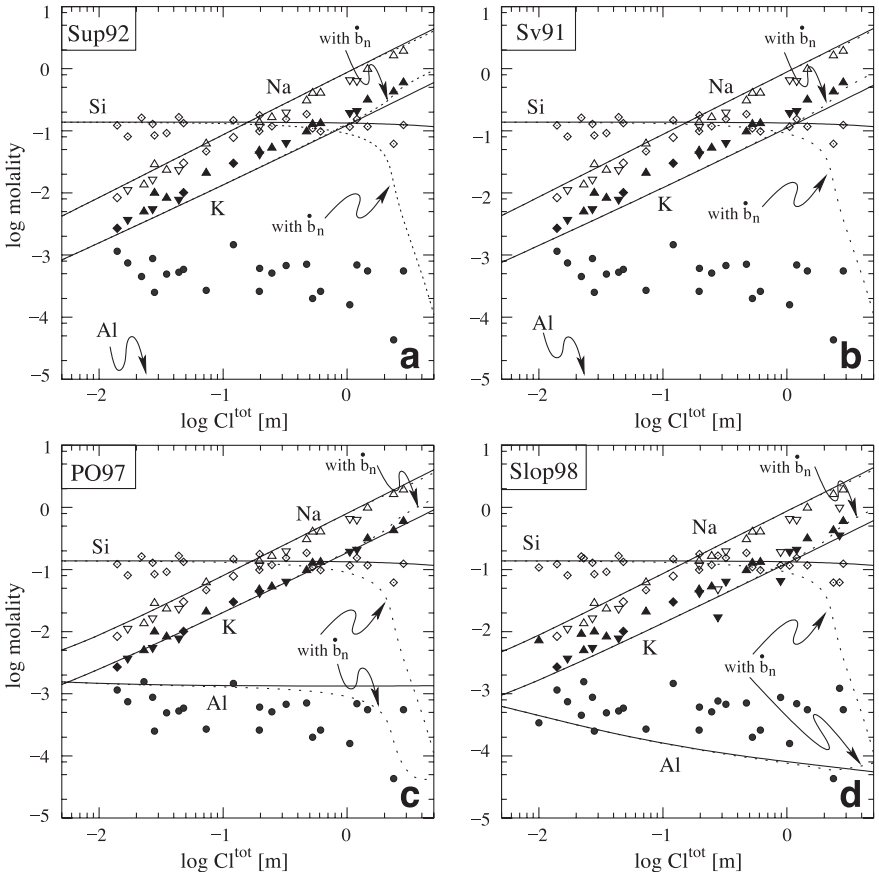

Fig. 4. (a–d) Comparison between experimental data (symbols) and thermodynamic models (curves). Total Si concentrations are well predicted by all databases. Only the Po97 data (d) predicts total Al concentrations in agreement with our experiments. The Al concentration for the Sup92 and Sv91 dataset is in the order of 10^{-19} to 10^{-13} molal increasing with total chloride concentration. Note that K concentrations are underestimated (except by Po97), while Na is slightly overestimated. Calculations were performed using the thermodynamic data for ordered 30 end member feldspars. The dashed curves use the Setchenow equation with $b_n = 1.4$ (NaCl) for neutral species. The predicted drop in Si concentration is not supported by the experiments.

and associated alkali-silica-hydroxide species $NaSi(OH)_5^0$ and $KSi(OH)_5^0$ have been proposed for basic and alkali-rich solutions (Anderson and Burnham, 1967). The latter species are expected to be unimportant, since all thermodynamic model calculations predict a slightly basic to acidic pH (from 7 to 4) for the experimental solutions. All data sets yield the same log K for the quartz solubility reaction (Table 4). This reflects the fact that a large experimental database is available for quartz solubility in pure water which is largely self consistent and was used for data retrieval (e.g. Walther and Helgeson, 1977; Manning, 1994).

6.2. Aluminum

Aluminum concentrations are underestimated by about 10 to 15 orders of magnitude by the Sup92 and Sverj91 databases (Fig. 4a,b). The Slop98 database underestimates Al concentrations by roughly one order of magnitude (Fig. 4c). It predicts a total solubility, which decreases slightly with increasing total chloride. Experimental Al concentrations agree well with the Po97 database (Fig. 4d). It includes a large set of Al species, including aluminum hydroxide species, and alkali aluminum hydroxides species.

Al is well known for its tendency to complex with hydroxide (Anderson and Burnham, 1967; Anderson et al., 1987; Woodland and Walther, 1987; Pascal and Anderson, 1989; Ragnarsdottir and Walther, 1985; Walther, 1986; Eugster and Baumgartner, 1987; Walther, 1997). Experiments on the solubility of corundum and alkali feldspars in basic alkali-metal solutions result in an increase in the solubility of several orders of magnitude (Anderson and Burnham, 1967; Anderson et al., 1987; Woodland and Walther, 1987; Pascal and Anderson, 1989). This has either been attributed to alkali aluminum complexing (e.g. Anderson et al., 1987; Woodland and Walther, 1987; Pascal and Anderson, 1989; Caiani et al., 1989; Chen et al., 1991; Pokrovskii and Helgeson, 1995) or to the presence of $Al(OH)_4^-$ or similar negatively charged aluminum hydroxide complexes (e.g. Walther, 1997). In contrast, aluminum chloride complexes have been reported in the literature only for conditions which are associated with extremely high hydrochloric acid concentrations (e.g. Baumgartner and Eugster, 1988). These interpretations are reflected in the choice of Al species available in each database (Table 4). The Po97 database includes the most extensive set of aluminum hydroxide and alkali-aluminum species.

All calculations performed for the assemblage albite + K-feldspar + andalusite + quartz at the P–T conditions of interest predict a slightly basic pH of 7 (neutral pH at 2 kbar and 650 °C = 5.6, see Table 4) to acidic pH values (pH 4) with increasing chloride content. The abundance of $Al(OH)_4^-$ species, or similar charged hydroxides, decreases with decreasing pH. Thus, a decrease in the Al concentration with an increasing total chloride concentration would be predicted, if a charged aluminum hydroxide species (e.g. $Al(OH)_4^-$) dominate the experimental solutions. Only a slight decrease is suggested by the experimental data. Hence, a different complex is likely at high chloride concentrations. Since Na^+ increases significantly, an alkali-aluminum complex is likely, as is predicted by the Po97 database (e.g. $NaAl(OH)_4^\circ$).

6.3. Alkali metals

The solubility of both alkali metals is proportional to the total chloride concentration (Fig. 4), indicating that both form associated chloride species. The total Na concentration is relatively insensitive to small variations of the albite hydrolysis reaction because the total Na is very close to the total Cl concentration. Hence, it is limited to higher concentrations by charge balance. The total K concentrations are significantly more sensitive to changes in the albite or the K-feldspar hydrolysis reaction, since it competes with Na for chlorine.

Initially, calculations were performed using the thermodynamic properties of pure ordered feldspars. In this case, the total Na content is slightly overestimated by all databases and the total K content is significantly underestimated by all databases except the PO97 dataset (Fig. 4a–d). Plotting the Po97 data for the K/Na ratio at linear scale, it is seen that the predicted values for the K/Na ratio are about 0.07–0.1 too low (Fig. 5). The use of disordered pure endmember feldspar properties further decreases the predicted K/Na ratio for all databases (Fig. 5). This is shown exemplary for the Po97 dataset in Fig. 5. Using the feldspar-mixing model of Fuhrman and Lindsley (1988), we calculated the activities from feldspar rim compositions (disordered feldspars). The use of these activities resulted in a slightly higher K/Na ratios than that for pure low feldspars (Fig. 6). In conclusion, none of the databases considered describe

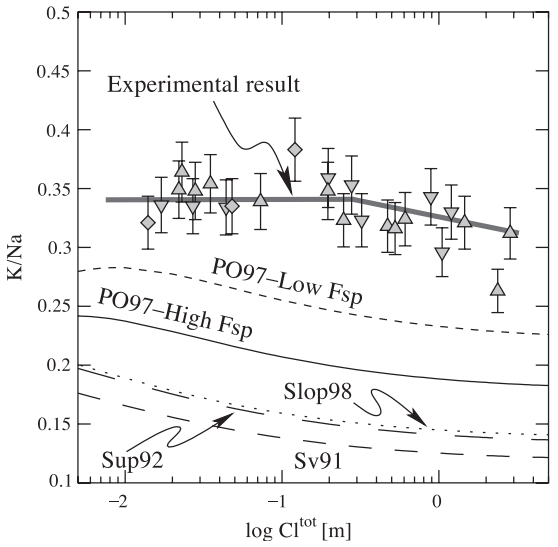

Fig. 5. A comparison of calculated (curves) and experimentally determined K/Na. The Po97 data best predicts the K/Na ratio. Note that if the feldspar is assumed to be disordered, the K/Na ratio decreases. High Fsp = disordered feldspars, Low Fsp = ordered feldspars.

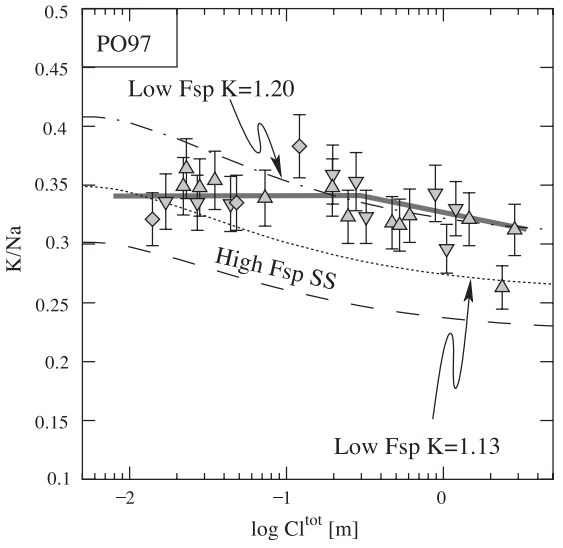

Fig. 6. Plot of K/Na vs. total chloride concentration of the fluid phase. A small increase in the equilibrium constant value for the K-feldspar dissolution reaction from 0.946 to a value between 1.13 and 1.20 results in good agreement between the predicted value and the observed. Accounting for the feldspar solid-solution properties using the Furman and Lindsley (1988) activity model together with disordered feldspar properties improves the fit slightly. High Fsp = disordered feldspars, High Fsp SS = solid solution of disordered feldspars, and Low Fsp = ordered feldspars.

the solubility of Na and K accurately. The best fit to the experimental data is obtained using thermodynamic data for high feldspars from the Po97 database in conjunction with the activity model of Fuhrman and Lindsley (1988).

As noted above, the K/Na ratio is very sensitive to the thermodynamic properties of the K-feldspar dissolution reaction (Table 4). An adjustment of the equilibrium constant for the K-feldspar dissolution reaction (Table 4) calculated for Po97 (log = 1.059) to a value of 1.13 fits the data reasonably well at low total chloride concentrations ($C^{tot} < 0.1$ m). At higher chloride concentrations ($Cl^{tot} = 0.1–3$ m), an adjustment of the log K to 1.20 gives a good fit. These adjustments of the equilibrium constant for the K-feldspar dissolution reaction are well within the uncertainties of the K-feldspar hydrolysis reaction. Nevertheless, the chloride dependence of the ratio is not reproduced in any case (Fig. 6).

The K/Na ratio dependence on chloride concentration can be used to investigate the speciation of K and Na in more detail. The ratio is sensitive to the speciation of the alkalis and the choice of the activity coefficient model for each species. To illustrate this,

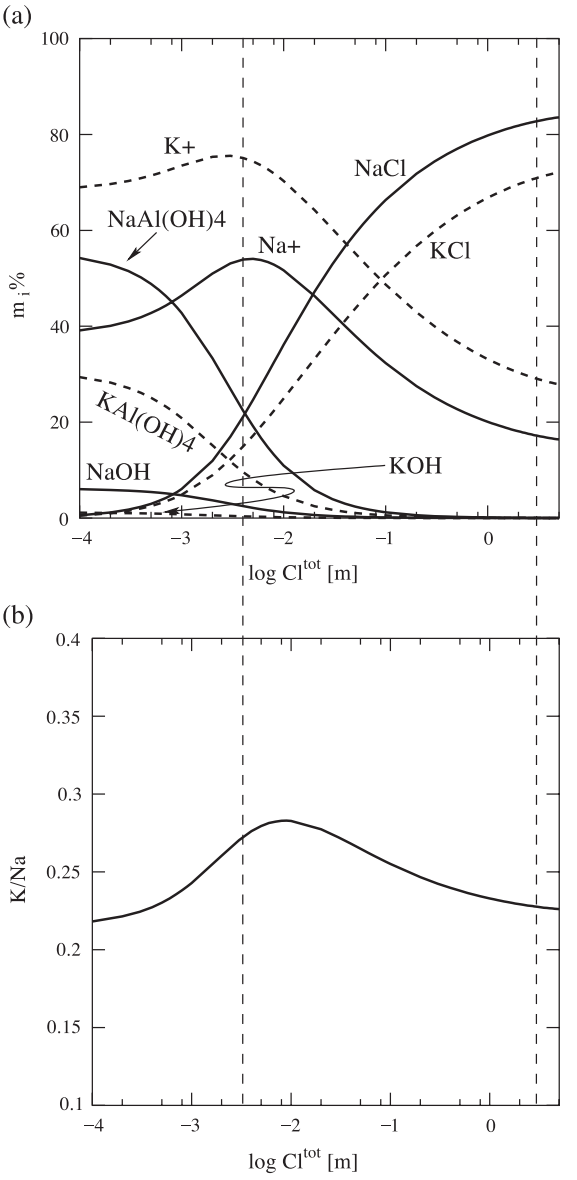

Fig. 7. Plot of speciation in the supercritical solution as a function of total chloride concentration. The speciation of metals dissolved in the supercritical solution is illustrated in (a). The relative percentage of each metal species compared to the total metal concentration for each metal is plotted. (b) shows that the K/Na ratios reflect any change in speciation.

consider the species distribution plot for alkalis predicted by the Po97 database (Fig. 7). The $\dot{b}$-term of the dominant species (NaCl, $\dot{b} = -0.109$ at 650 °C and 2 kbar; Oelkers and Helgeson, 1991) was used together with a unit activity coefficient for neutral species. An initial increase in the K/Na ratio reflects a decrease in the percentage of the alkali-aluminum-hydroxide species, while a subsequent decrease in this ratio is due to increasing association of the alkali metals with chloride (Fig. 7).

The experimental K/Na line is horizontal at low chloride concentrations (up to 0.4 m Cl^{tot}; Figs. 2 and 5). A slight decrease is indicated towards higher chloride concentrations. This suggests that a single set of species dominate over this chloride range. Comparison with the calculated speciation (Po97) would suggest that either NaCl and KCl are less stable than predicted, resulting in the dominance of K^+ and Na^+, or alternatively, NaCl and KCl are more stable, and prevail over Na^+ and K^+ towards lower chloride concentrations. Changing either the dissociation reaction constants for the alkali chloride complexes or the activity coefficients would achieve this. For example, a very large Setchenow coefficient would suppress the formation of the neutral complexes, and K^+ and Na^+ would be favoured.

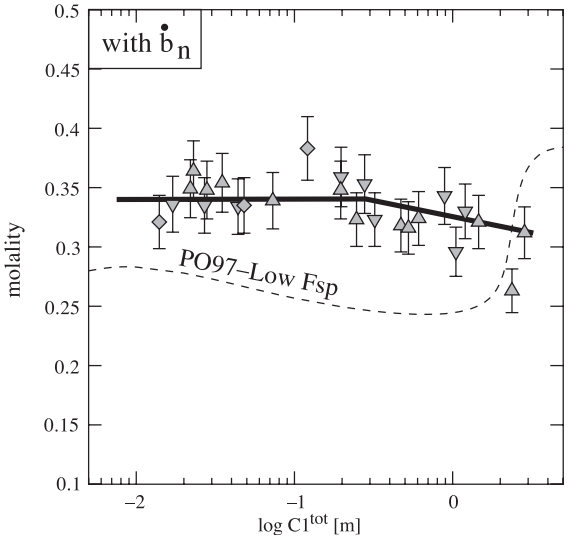

Fig. 8. Comparison between the experimentally determined K/Na ratio from this study and various models' predictions. The experimentally determined K/Na ratio decreases slightly with increasing total chloride, while model calculations predict a significant increase when the Setchenow coefficient ($\dot{b}_n = 1.4$), published by Oelkers and Helgeson (1991), for NaCl is used. Calculations have been performed with endmember ordered feldspars (Low Fsp).

To illustrate the influence of the Setchenow coefficient on the K/Na ratio, we recalculated Fig. 5 with $\dot{b} = -0.109$ for charged species (Oelkers and Helgeson, 1990) and $\dot{b}_n = 1.4$ for neutral NaCl (Oelkers and Helgeson, 1991), which is that of the dominant solute (Fig. 8). At very low chloride concentrations ($Cl^{tot} < 0.05$), the sodium-aluminum-hydroxide species is dominant, followed by Na^+, K^+, and finally NaCl, KCl the dominant species. At higher chloride concentration, the associated NaCl and KCl species are destabilized by the large Setchenow coefficient and Na^+ is the dominant species. This speciation change is visible in Fig. 8 by the sharp increase of the K/Na ratio at Cl^{tot} of about 1–2 molal. Since our experimentally determined data show a completely different trend, we conclude that the Setchenow coefficient of 1.4 is overestimated and we recommend the use of unit activity coefficient ($\dot{b}_n \cong 0$) for neutral species with the used activity model in this study.

7. Conclusions

The presented experiments at 650 °C and 2 kbar confirm that Na and K linearly increase with total chloride concentration as expected (Table 2). Na solubility increases from ~ 0.01 molal at 0.01 molal Cl^{tot} to ~ 1.9 molal at 2.9 molal Cl^{tot}; K from ~ 0.005 to ~ 0.6 molal. The shape of the K/Na ratio with increasing Cl^{tot} indicate that K and Na speciations are not changing dramatically for chloride concentrations between 0.1 and 3 molal. This is in agreement with results reported by Hauzenberger et al. (2001) for solubility experiments done at 600 °C and 2 kbar. Small differences between the predicted and the experimental chloride dependence of the K/Na ratio are apparent. This suggests that the speciation is not yet adequate for alkali metals. The effect of the Setchenow $\dot{b}_n$ parameter ($\dot{b}_n = 1.4$ for NaCl) as given by Oelkers and Helgeson (1991) on the total K and Na concentration is to increase the K/Na ratios at high Cl concentrations

(Fig. 8). This is not observed experimentally. This indicates that the $\dot{b}_n$ parameter for neutral alkali species is overestimated.

The comparison of our experimental results with various thermodynamic models for aqueous solutions indicates that the Po97 database (see Tables 3 and 4) best describes the experimental data at 650 °C and 2 kbar. The best fit is obtained by using disordered feldspar properties, together with the activity model for feldspars of Fuhrman and Lindsley (1988). This would suggest that the precipitation reactions are faster than the dissolution reactions, once the precipitate nucleated. Hence, they determine the solubility in our experiments.

The experiments support the Al speciation scheme implemented in the Po97 database. Both aluminum hydroxide and alkali aluminum hydroxide species are needed to accurately describe the solubility of Al in aqueous solutions. The experimentally determined Al solubility is in the range of ~ 0.0015 to ~ 0.0007 molal. Si concentrations are well predicted in these complicated experimental fluids and are found to be ~ 0.13 molal.

The results from this experimental study and its comparison with current, relevant thermodynamic databases are encouraging. The success of predicting the total metal concentration in the complex chloride solutions suggests that solubility calculations can be performed with some confidence for metamorphic solutions containing abundant alkali chloride and other cations. Based on the above discussion, we recommend to use the Po97 database, with the extended Debye–Hückel equation and unit activity coefficients for neutral aqueous complexes.

Acknowledgements

This study is part of the PhD thesis research conducted by Dr. T. Pak at the University of Wisconsin-Madison. This work was supported by NSF grants EAR-92-57160, EAR-93-16504 and EAR-96-14649 to LPB. We would like to thank Dr. V.A. Pokrovskii and Dr. D.E. Harlov for insightful criticism and constructive reviews of the manuscript. Dr. E. Oelkers is thanked for comments that led to a significant improvement of the manuscript. **[EO]**

References

Ague, J.J., 1991. Evidence for major mass transfer and volume strain during regional metamorphism of pelites. Geology 19, 855–858.

Ague, J.J., 1994a. Mass transfer during Barrovian metamorphism of pelites, South-Central Connecticut: I. Evidence for changes in composition and volume. Am. J. Sci. 294, 989–1057.

Ague, J.J., 1994b. Mass transfer during Barrovian metamorphism of pelites, South-Central Connecticut: II. Channelized fluid flow and the growth of staurolite and kyanite. Am. J. Sci. 294, 1061–1134.

Ague, J.J., 1997a. Compositional variations in metamorphosed sediments of the Littleton Formation, New Hampshire. Am. J. Sci. 297, 440–449.

Ague, J.J., 1997b. Crustal mass transfer and index mineral growth in Barrow's garnet zone, Northeast Scotland. Geology 25, 73–76.

Anderson, G.M., Burnham, C.W., 1963. Effect of chloride on the composition of pegmatite fluids. Geol. Soc. Am. Spec. Publ., 104.

Anderson, G.M., Burnham, C.W., 1967. Reactions of quartz and corundum with aqueous chloride and hydroxide solutions at high temperatures and pressures. Am. J. Sci. 265, 12–27.

Anderson, G.M., Burnham, C.W., 1983. Feldspar solubility and the transport of aluminum under metamorphic conditions. Am. J. Sci. 283-A, 283–297.

Anderson, G.M., Pascal, M.L., Rao, J., 1987. Aluminum speciation in metamorphic fluids. In: Helgeson, H.C. (Ed.), Chemical Transport in Metasomatic Processes. Reidel, Dordrecht, pp. 297–321.

Banks, D.A., Davies, G.R., Yardley, B.W.D., McCaig, A.M., Grant, N.T., 1991. The chemistry of brines from an Alpine thrust system in the central Pyrenees; an application of fluid inclusion analysis to the study of fluid behaviour in orogenesis. Geochim. Cosmochim. Acta 55, 1021–1030.

Barnes, H.L., 1981. Measuring thermodynamically interpretable solubilities at high pressures and temperatures. In: Rickard, D., Wickman, F. (Eds.), Chemistry and Geochemistry of Solutions at High Temperatures and Pressures. Physics and Chemistry of the Earth, vol. 13/14. Pergamon, New York, pp. 321–343.

Baumgartner, L.P., 1992. Experimental support for a sodium chloride species with Cl:Na>1 from solubility data on the assemblage albite + andalusite + quartz. Geol. Soc. Am. Abstr. 24/7, A207.

Baumgartner, L.P., Eugster, H.P., 1988. Experimental determination of corundum solubility and Al-speciation in supercritical H_2O–HCl solutions. Geol. Soc. Am. Abstr. 20/7, 191.

Beswick, A.E., 1973. An experimental study of alkali metal distributions in feldspars and micas. Geochim. Cosmochim. Acta 37, 183–208.

Brimhall, G.H., Crerar, D.A., 1987. Ore fluids: magmatic to supergene. In: Carmichael, I.S.E., Eugster, H.P. (Eds.), Thermodynamic Modeling of Geological Materials: Minerals, Fluids and Melts. Mineralogical Society of America. Reviews in Mineralogy, vol. 17, pp. 235–322.

Bockris, J.O'M., Reddy, A.K.N., 1970. Modern Electrochemistry. Plenum, New York, p. 1432.

Born, V.M., 1920. Volumen und Hydratationswärme der Ionen. Phys. Z. 1, 45–48.

Burnham, C.W., 1967. Hydrothermal fluids at the magmatic stage. In: Barnes, H.L. (Ed.), Geochemistry of Hydrothermal Ore Deposits. Holt, Rinehart and Winston, New York, pp. 34–76.

Caiani, P., Conti, G., Gianni, P., Matteoli, E., 1989. Apparent molar heat capacity and relative enthalpy of aqueous sodium hydroxoaluminate between 323 and 523 K. J. Solution Chem. 18, 447–461.

Chen, Q., Xu, Y., Helper, L.G., 1991. Calorimetric study of the digestion of gibbsite, $Al(OH)_3$(cr), and thermodynamics of aqueous aluminate ion, $Al(OH)_4^-$(aq). Can. J. Chem. 69, 1685–1690.

Dipple, G.M., Ferry, J.M., 1992. Metasomatism and fluid flow in ductile fault zones. Contrib. Mineral. Petrol. 112, 149–164.

Dipple, G.M., Wintsch, R.P., Andrews, M.S., 1990. Identification of the scales of differential element mobility in a ductile fault zone. J. Metamorph. Geol. 8, 645–661.

Eugster, H.P., Baumgartner, L.P., 1987. Mineral solubilities and speciation in supercritical metamorphic fluids. In: Carmichael, I.S.E., Eugster, H.P. (Eds.), Thermodynamic Modeling of Geological Materials: Minerals, Fluids and Melts, Mineralogical Society of America. Reviews in Mineralogy, vol. 17, pp. 367–403.

Eugster, H.P., Chou, I.-M., Wilson, G.A., 1987. Mineral solubility and speciation in supercritical chloride fluids. In: Ulmer, G.C., Barnes, H.L. (Eds.), Hydrothermal Experimental Techniques. Wiley, New York, pp. 1–19.

Ferry, J.M., 1988. Infiltration-driven metamorphism in northern New England, USA. J. Petrol. 29, 1121–1159.

Frantz, J.D., Marshall, W.L., 1984. Electrical conductance and ionization constants of salts, acids, and bases in supercritical aqueous fluids: I. Hydrochloric acid from 100 °C to 700 °C and at pressures to 4000 bars. Am. J. Sci. 284, 651–667.

Fuhrman, M.L., Lindsley, D.H., 1988. Ternary-feldspar modeling and thermometry. Am. Mineral. 73, 201–215.

Gunter, W.D., Eugster, H.P., 1980. Mica–feldspar equilibrium in supercritical alkali chloride solutions. Contrib. Mineral. Petrol. 66, 271–281.

Hauzenberger, C.A., Pak, T.M., Baumgartner, L.P., 2001. Experimental study on the solubility of the "model"-pelite mineral assemblage albite + K-feldspar + andalusite + quartz in supercritical chloride rich aqueous solutions at 0.2 GPa and 600 °C. Geochim. Cosmochim. Acta 65, 4493–4507.

Helgeson, H.C., Delaney, J.M., Nesbit, H.M., Bird, D.K., 1978. Summary and critique of the thermodynamic properties of rock-forming minerals. Am. J. Sci. 278A, 1–229.

Helgeson, H.C., Kirkham, D.H., Flowers, G.C., 1981. Theoretical prediction of the thermodynamic behavior of aqueous electrolytes at high pressures and temperatures: IV. Calculation of activity coefficients, osmotic coefficients and apparent molal and relative partial molal properties to 600 °C and 5 kb. Am. J. Sci. 281, 1249–1516.

Hemley, J.J., 1959. Some mineralogical equilibrium in the system K_2O-Al_2O_3-SiO_2-H_2O. Am. J. Sci. 257, 241–270.

Hemley, J.J., 1967. Stability relations of pyrophyllite, andalusite, and quartz at elevated pressures and temperatures. EOS Abstr. 48/1, 224.

Holdaway, M.J., 1971. Stability of andalusite and the aluminium silicate phase diagram. Am. J. Sci. 271, 97–131.

Holland, T.J.B., Powell, R., 1998. An internally consistent thermodynamic data set for phases of petrological interest. J. Metamorph. Geol. 16, 309–343.

Hückel, E., 1925. Zur Theorie konzentrierter wässeriger Lösungen starker Elektrolyte. Phys. Z. 26, 93–147.

Johnson, J.W., Oelkers, E.H., Helgeson, H.C., 1992. SUPCR92: a software package for calculating the standard molal thermodynamic properties of mineral, gases, aqueous species, and reactions from 1 to 5000 bars and 0 to 1000 °C. Comput. Geosci. 18, 899–947.

Lagache, M., Weisbrod, A., 1977. The system two alkali feldspars-KCl-NaCl-H_2O at moderate to high temperatures and low pressures. Contrib. Mineral. Petrol. 62, 77–101.

Lasaga, A.C., Rye, D.M., Luettge, A., Bolton, E.W., 2001. Calculation of fluid fluxes in Earth's crust. Geochim. Cosmochim. Acta 65, 1161–1185.

Manning, C.E., 1994. The solubility of quartz in H_2O in the lower crust and upper mantle. Geochim. Cosmochim. Acta 58, 4831–4839.

Manning, C.E., 1997. Coupled reaction and flow in subductions zones: silica metasomatism in the mantle wedge. In: Jamtveit, B., Yardley, B.W.D. (Eds.), Fluid Flow and Transport in Rocks. Chapman and Hall, Dordrecht, pp. 139–147.

Manning, C.E., 2001. Experimental studies of fluid–rock interaction at high pressure: the role of polymerization and depolymerization of solutes. 11th Annual V.M. Goldschmidt Conference, 3807.pdf.

Martin, R.F., 1969. The hydrothermal synthesis of low albite. Contrib. Mineral. Petrol. 23, 323–339.

Montoya, J.W., Hemley, J.J., 1975. Activity relations and stabilities in alkali feldspar and mica alteration reactions. Econ. Geol. 70, 577–583.

Oelkers, E.H., Helgeson, H.C., 1990. Triple-ion anions and polynuclear complexing in supercritical electrolyte solutions. Geochim. Cosmochim. Acta 54, 727–738.

Oelkers, E.H., Helgeson, H.C., 1991. Calculation of activity coefficients and degrees of formation of neutral ion pairs in supercritical electrolyte solutions. Geochim. Cosmochim. Acta 55, 1235–1251.

Oelkers, E.H., Helgeson, H.C., 1993. Calculation of dissociation constants and the relative stabilities of polynuclear clusters of 1:1 electrolytes in hydrothermal solutions at supercritical pressures and temperatures. Geochim. Cosmochim. Acta 57, 2673–2697.

Oelkers, E.H., Helgeson, H.C., Shock, E.L., Sverjensky, D.A., Johnson, J.W., Porkrovskii, V.A., 1995. Summary of the apparent standard partial molal Gibbs Free Energies of formation of aqueous species, minerals and gases at pressures 1 to 5000 bars and temperatures 25 to 1000 degrees C. J. Phys. Chem. Ref. Data 24, 1401–1560.

Orville, P.M., 1963. Alkali ion exchange between vapor and feldspar phases. Am. J. Sci. 261, 201–239.

Orville, P.M., 1967. Unit-cell parameter of the microcline-low albite and sanidine-high albite solid solution series. Am. Mineral. 52, 55–86.

Pascal, M.L., Anderson, G.M., 1989. Speciation of Al, Si, and K in supercritical solutions: experimental study and interpretation. Geochim. Cosmochim. Acta 53, 1843–1855.

Pokrovskii, V.A., Helgeson, H.C., 1995. Thermodynamic properties of aqueous species and the solubilities of minerals at high pressures and temperatures: the system Al_2O_3-H_2O-NaCl. Am. J. Sci. 295, 1255–1342.

Pokrovskii, V.A., Helgeson, H.C., 1997. Calculation of the standard partial molal thermodynamic properties of KCl and activity coefficients of aqueous coefficients of aqueous KCl at temperatures and pressures to 1000 °C and 5 kbar. Geochim. Cosmochim. Acta 61, 2175–2183.

Popp, R.K., Frantz, J.D., 1980. Mineral-solution equilibrium: III. The system Na_2O-Al_2O_3-SiO_2-H_2O-HCl. Geochim. Cosmochim. Acta 44, 1029–1038.

Ragnarsdottir, K.V., Walther, J.V., 1985. Experimental determination of corundum solubilities in pure water at 400 to 700 °C and 1 to 3 kbar. Geochim. Cosmochim. Acta 49, 2109–2115.

Ridley, J.R., Diamond, L.W., 2000. Fluid chemistry of orogenic lode gold deposits and implications for genetic models. Rev. Econ. Geol. 13, 141–162.

Roedder, E., 1984. Fluid inclusions. Mineral. Soc. Am. Rev. Mineral. 12 (644 pp.).

Roselle, G.T., Baumgartner, L.P., 1995. Experimental determination of the anorthite solubility and calcium speciation in supercritical chloride solutions at 2 kbar from 400 ° to 600 °C. Geochim. Cosmochim. Acta 59, 1539–1549.

Roux, J., Hovis, G.L., 1996. Thermodynamic mixing models for muscovite–paragonite solutions based on solution calorimetric and phase equilibrium data. J. Petrol. 37, 1241–1254.

Rudert, V., Chou, I.M., Eugster, H.P., 1976. Temperature gradients in rapid-quench cold-seal pressure vessels. Am. Mineral. 61, 1012–1015.

Setchenow, M., 1892. Action de l'acide carbonique sur les solutions des sels acides forts. Ann. Chem. Phys. 25, 225–270.

Shade, J.W., 1974. Hydrolysis reactions in the SiO_2 excess portion of the system K_2O-Al_2O_3-SiO_2-H_2O in chloride fluids at magmatic conditions. Econ. Geol. 69, 218–228.

Shinohara, H., Fujimoto, K., 1994. Experimental study in the system albite-andalusite-quartz-NaCl-HCl-H_2O at 600 °C and 400 to 2000 bars. Geochim. Cosmochim. Acta 58, 4857–4866.

Shock, E.L., 1998. An updated and augmented version (slop98.dat) of the original SUPCRT92 database (sprons92.dat). http://geology.asu.edu/people/faculty/shock/.

Shock, E.L., Helgeson, H.C., 1988. Calculation of thermodynamic and transport properties of aqueous species at high temperatures and pressures: correlation algorithms for ionic species and equation of state predictions to 5 kb and 1000 °C. Geochim. Cosmochim. Acta 53, 2009–2036.

Shock, E.L., Helgeson, H.C., Sverjensky, D.A., 1989. Calculation of the thermodynamic and transport properties of aqueous species at high pressures and temperatures: standard partial molal properties of inorganic neutral species. Geochim. Cosmochim. Acta 53, 2157–2183.

Shock, E.L., Oelkers, E.H., Johnson, J.W., Sverjensky, D.A., Helgeson, H.C., 1992. Calculation of the thermodynamic properties of aqueous species at high pressures and temperatures: effective electrostatic radii, dissociation constants, and standard partial molal properties to 1000 °C and 5 kbar. J. Chem. Soc. Faraday Trans. 88, 803–826.

Shock, E.L., Sassani, D.C., Willis, M., Sverjensky, D.A., 1997. Inorganic species in geologic fluids: correlation among standard molal thermodynamic properties of aqueous ions and hydroxide complexes. Geochim. Cosmochim. Acta 61, 907–950.

Spear, F.S., 1993. Metamorphic phase equilibrium and pressure–temperature–time paths. Mineral. Soc. Am. Monogr. (799 pp.).

Sterner, S.M., Hall, D.L., Bodnar, R.J., 1988. Synthetic fluid inclusions: V. Solubility relations in the system NaCl-KCl-H_2O under vapor-saturated conditions. Geochim. Cosmochim. Acta 52, 989–1006.

Sterner, M.S., Chou, I.-M., Downs, R.T., Pitzer, K.S., 1992. Phase relations in the system NaCl-KCl-H_2O: V. Thermodynamic *PTX* analysis of solid–liquid equilibrium at high *P* and *T*. Geochim. Cosmochim. Acta 56, 2295–2309.

Sverjensky, D.A., Hemley, J.J., D'Angelo, W.M., 1991. Thermodynamic assessment of hydrothermal alkali feldspar–mica–aluminosilicate equilibrium. Geochim. Cosmochim. Acta 55, 989–1004.

Sverjensky, D.A., Shock, E.L., Helgeson, H.C., 1997. Prediction of the thermodynamic properties of aqueous metal complexes to 1000 °C and 5 kb. Geochim. Cosmochim. Acta 61, 1359–1412.

Tanger IV, J.C., Helgeson, H.C., 1988. Calculation of the thermodynamic and transport properties of aqueous species at high pressures and temperatures. Revised equations of state for the standard partial molal properties of ions and electrolytes. Am. J. Sci. 288, 19–98.

Tuttle, O.F., 1949. Two pressure vessels for silicate–water studies. Geol. Soc. Amer. Bull. 60, 1727–1729.

Vidale, R., 1983. Pore solution compositions in a pelitic system at high temperatures, pressures, and salinities. Am. J. Sci. 283-A, 298–313.

Walther, J.V., 1986. Mineral solubilities in supercritical H_2O solutions. Pure Appl. Chem. 58, 1585–1598.

Walther, J.V., 1997. Experimental determination and interpretation of the solubility of corundum in H_2O between 350° and 600 °C from 0.5 to 2.2 kbar. Geochim. Cosmochim. Acta 61, 4955–4964.

Walther, J.V., Helgeson, H.C., 1977. Calculation of the thermodynamic properties of aqueous silica and the solubility of quartz and its polymorphs at high pressures and temperatures. Am. J. Sci. 277, 1315–1351.

Walther, J.V., Orville, P.M., 1983. The extraction-quench technique for determination of the thermodynamic properties of solute complexes: application to quartz solubility in fluid mixtures. Am. Mineral. 68, 731–741.

Walther, J.V., Woodland, A.B., 1993. Experimental determination and interpretation of the solubility of the assemblage microcline, muscovite, and quartz in supercritical H_2O. Geochim. Cosmochim. Acta 57, 2431–2437.

Wellman, T.R., 1970. The stability of sodalite in a synthetic syenite plus aqueous chloride fluid system. J. Petrol. 11, 49–71.

Wilson, G.A., Eugster, H.P., 1990. Cassiterite solubility and tin speciation in supercritical chloride solutions. In: Spencer, R.J., Chou, I.M. (Eds.), Fluid–Mineral Interactions: A Tribute to

H.P. Eugster. Geochemical Society Special Publications, vol. 2, pp. 179–198.

Wintsch, R.P., Merino, E., Blakery, R.F., 1980. Rapid-quench hydrothermal experiments in dilute chloride solutions applied to the muscovite–quartz–sanidine equilibrium. Am. Mineral. 65, 1002–1011.

Woodland, A.B., Walther, J.V., 1987. Experimental determination of the solubility of the assemblage paragonite, albite and quartz in supercritical H_2O. Geochim. Cosmochim. Acta 51, 365–372.

Wolery, T.J., 1979. Calculation of chemical equilibrium between aqueous solutions and minerals: the EQ3/6 software package. Lawrence Livermore National Laboratory, URCL-52658.